Modelling the optical properties of microstructured optical fibres

Tanya M. Monro, Vittoria Finazzi, Joanne C. Baggett and David J. Richardson
Optoelectronics Research Centre, University of Southampton, UK
tmm@orc.soton.ac.uk

Abstract

The presence of wavelength-scale holes in a microstructured optical fibres leads to challenges in the accurate modelling of their optical properties. A wide variety of techniques can be used, ranging from effective step-index fibre models to approaches that incorporate the full complexity of the fibre cross-section. Here these approaches will be reviewed and assessed in terms of their suitability for modelling optical properties of microstructured optical fibres such as their mode area, chromatic dispersion, form birefringence and confinement loss. Some of the issues associated with designing and modelling practical microstructured fibres are discussed.

1 Introduction

A new class of optical fibre has emerged in recent years: the microstructured fibre [1]. These fibres guide light by means of an arrangement of air-holes that run along the fibre, and some examples are shown in Fig. 1 (note that the hole-to-hole spacing is Λ and d is the hole diameter). In these fibres, light can be guided using either one of two quite different mechanisms. Ref. [2] originally proposed that light could be guided via photonic band gap effects; and this guidance mechanism was demonstrated in Ref. [3]. The second means of guiding light makes fewer demands on the fibre geometry: in fibres like those shown in Fig. 1, light is guided due to an effective average index difference between the solid core and the region containing air holes, which acts as the cladding. This *effective index* guidance is routinely observed in these fibres, and their basic operation does not depend on having a periodic array of holes; in fact the holes can even be arranged randomly [4]. Such fibres are generally labelled *holey fibres* (HFs) or *microstructured fibres*. HFs can be made from a single material, and to date, the majority of these fibres have been fabricated from pure silica. Recently active silica HFs with Yb^{3+}-doped cores [5, 6] have been developed, HFs have also been fabricated in chalcogenide glass [7] and in polymers [8].

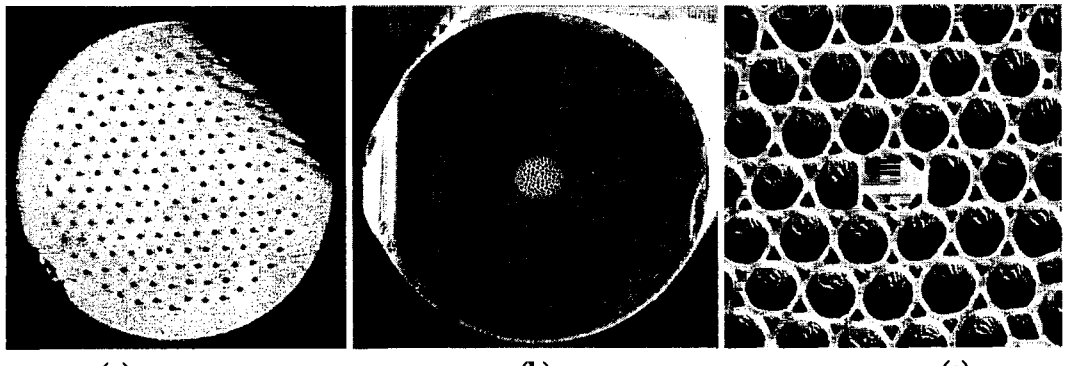

(a) (b) (c)

Figure 1: (a) Large mode area silica HF with $\Lambda = 7.6\,\mu$m, $d = 1.7\,\mu$m (b) small mode area silica HF ($\Lambda = 1.5\,\mu$m) (c) A highly-birefringent silica holey fibre with a Yb^{3+}-doped core (core dimensions $2.6 \times 1.5\,\mu$m)

The optical properties of these fibres are determined by the configuration of air holes that forms the cladding region, and HFs can have mode areas ranging over three orders of magnitude by scaling the dimensions of the structure. Mode areas from $1\,\mu m^2$ to over $500\,\mu m^2$ at 1550nm are possible [9]. Small mode area fibres can be used for devices based on nonlinear effects [10], whereas the large mode fibres allow high power delivery [11]. In

addition, these fibres can exhibit optical properties not readily attainable in conventional fibres, including endlessly single-mode guidance [12] and anomalous dispersion well below 1.3 microns [13]. Dispersion and birefringence are two properties that can depend strongly on the cladding configuration, particularly when the hole-to-hole separation is small. By exploiting the innate flexibility provided by the choice of hole arrangement, it is thus possible to design fibres with a wide range of characteristics. For example, poled HFs can offer advantages for second harmonic generation (SHG) [14] because they allow more freedom for producing optimum mode properties at second harmonic and pump wavelengths than conventional poled optical fibres, resulting in up to four orders of magnitude improvement in SHG efficiency relative to conventional fibres. Note that the modes of single-material HFs are leaky modes because the core index is the same as that beyond the finite holey cladding, and for some designs this can lead to significant confinement loss [15].

In order to take advantage of the tailorable optical properties of HFs, it is crucial to use accurate methods for predicting their properties. A range of theoretical techniques exist for modelling the optical properties of HFs, and they are reviewed in Section 2. Sections 3 and 4 outline some of the additional challenges associated with designing and modelling small and large-mode area HFs respectively.

2 Overview of modelling

2.1 Effective index methods

The first technique that was applied to HFs was the *effective index method.* The effective index model approximates the HF structure with an *equivalent* step-index fibre. Once the equivalent step-index fibre has been defined, standard results for conventional fibres can be applied.

Despite ignoring the spatial distribution of the refractive index profiles within HFs, the effective index method can provide some insight into HF operation. For example, it correctly predicts the endlessly single-mode guidance regime in small-hole HFs. However this reduced model cannot accurately predict modal properties such as dispersion or birefringence that depend critically on the hole configuration [9]. In the extreme case of small-scale HFs with very large air filling fractions, the glass filaments within the cladding can be significantly smaller than the wavelength, and so the complex geometry can be approximated using the analogy of a glass rod suspended in air. For example, see Ref. [16], which uses this approach to predict that such fibres can exhibit large normal dispersion at telecommunications wavelengths.

However, the difficulty in using this approach arises from how the equivalent properties of the step-index fibre are defined. One method for making this choice is described in Ref [12]. In this work, the core index of the step-index fibre is taken to be that of silica, the cladding index is taken to be the effective index of the fundamental space-filling mode of the (infinite) cladding and the core diameter is chosen to be proportional to Λ. These results can be made to agree well with full simulations via appropriate choice of this constant of proportionality. However, for different structures or wavelengths, different choices can become necessary. This restricts the usefulness of this approach, since it is typically necessary to determine the best choice of equivalent structure by referring to results from a more complete numerical model. Ref. [17] explores the possibility of choosing the step-index fibre parameters in a more general fashion by allowing a wavelength dependent core or cladding index. However, to date no entirely satisfactory method for ascribing parameters to the equivalent fibre has been found.

2.2 Structural methods

As mentioned above, in order to accurately model HFs it is typically necessary to account for the complex spatial distribution of air holes that define the cladding. In this section, the techniques that have been developed to do this are outlined. A range of these techniques have also been successfully applied to photonic band gap fibres, although this is not discussed further here for brevity. Note that when the effective index contrast between core and cladding regions is large, the weak-guidance (scalar) approximation breaks down, leading to inaccurate results, and it is often necessary to adopt a vectorial method that includes polarisation effects. This is typically necessary when the air-filling fraction of the cladding is large [18]. Vectorial methods are also appropriate for asymmetric structures. Most of the techniques described in this section can be implemented in both scalar and vector forms.

Beam propagation methods (BPM) can be used to calculate the modal properties of HFs. For example, Ref. [19] uses a commercial BPM package to investigate a modified conventional Ge-doped fibre in which 6 large area holes have been added around the doped core region. A Bragg grating written in the core of the fibre was used to investigate the cladding modes of the structure, and good agreement with the BPM predictions was found.

Another candidate approach is the plane wave method [20], which is an adaptation of the method commonly used to investigate the photonic band structures of photonic crystals. In this technique, the modal fields and the refractive index profile are both decomposed into plane waves. In this way, any complex spatial index distribution can be described accurately. Provided that enough Fourier coefficients are included, this approach can yield accurate predictions for modal characteristics such as the number of modes supported by the fibre, the mode shape and size, and the dispersion properties. A similar approach is the variational plane-wave method in Ref. [21]. One disadvantage of these approaches is that they make no assumptions about the spatial distribution of the electric or magnetic fields. Hence they take no advantage of the localisation of the guided modes, and many terms need to be used in the field decompositions for accuracy. Typical implementations of the plane-wave method define the refractive index in a restricted region and use periodic boundary conditions to extend the structure (the super-cell approach). This additional periodicity restricts its applicability, since HFs do not need to be periodic.

An alternate approach was developed by Mogilevtsev et al. [22] which describes the modal fields using localised functions. This technique takes advantage of mode localisation, and so is more efficient than the plane-wave methods, it however cannot be accurate unless the refractive index is also represented well.

A hybrid approach, which combines some of the best features of the techniques described above was developed in Refs [9, 18, 23], and some recent extensions to this approach are outlined briefly here. In Refs [9, 18], the air hole lattice is described using a plane-wave decomposition, as in the plane-wave techniques described above, and the solid core and the modal fields are described using localised functions. This allows for an efficient description, particularly for idealised periodic structures, since only symmetric terms need to be used in the expansions. In order to model HFs with asymmetric profiles or to obtain accurate predictions for higher-order modes, it is necessary to extend this approach to use a complete basis set, and this was done in Ref. [23]. When more complex fibre profiles are considered, the advantages of describing the localised core separately from air holes is diminished, and the best combination of efficiency and accuracy is obtained by describing the entire refractive index distribution using a plane-wave expansion, while using localised functions only for the modal fields. This general implementation of this hybrid approach can be used to explore the full range of HF structures and modes, and can predict the properties of actual HFs by using SEM photographs to define the refractive index profile in the model [24]. This allows the deviations in optical properties which are caused by the subtle changes in structure to be explored.

In this implementation, the entire transverse refractive index profile is described using a plane-wave expansion, and the Fourier coefficients are evaluated by performing overlap integrals, which only need to be calculated once for any given structure. The modal electric field is expanded into orthonormal Hermite-Gaussian functions (both even and odd functions are included). Typically only a limited number of terms are required to reconstruct the observed modal profiles. These decompositions can be used to convert the vector wave equation into a simple eigenvalue problem (as in the plane wave method) that can be solved for the modal propagation constants and fields. In order to solve the system, a number of overlap integrals between the various basis functions need to be evaluated. For the choice of decompositions made here, these overlaps can be performed analytically, which is a significant advantage of this approach.

Most of the modelling done to date has considered ideal hexagonal arrangements of air holes. Group theory arguments can be used to show that all symmetric structures with higher than 2-fold symmetry are not birefringent [25]. However, as the techniques described in this Section perform calculations based on a Cartesian grid, they typically predict a small degree of birefringence that can be reduced (but not eliminated) by using a finer grid. When modelling asymmetric structures with a form birefringence that is significantly larger than this false birefringence, it is possible to make reasonably accurate predictions for fibre birefringence (see for example Section 3).

2.3 Predicting confinement loss

As mentioned earlier, for single-material HFs, it can be important to have a means of predicting confinement loss, since all guided modes are intrinsically leaky modes. Even in doped HFs, which can have true bound modes, it can be important to understand the leakage characteristics of cladding modes which can themselves be leaky. The confinement loss associated with a given fibre mode can be extracted from the imaginary part of the modal propagation constant. Apart from the BPM approach, none of the techniques described in Section 2.2 can (in their current forms) calculate complex propagation constants.

One technique that has recently been applied to this problem is the multipole approach [15], and some sample results from this method are given in Section 3 for small-core fibres. This approach is suitable for studying effects caused by the finite cladding region because it does not make use of periodic boundary conditions. Another advantage of this method is that it calculates the modal fields using decompositions that are based in each of the cladding air holes, and so it avoids the false birefringence problems associated with using a Cartesian coordinate

system described above. For this reason, this method is also particularly well suited to exploring the symmetry properties of HFs. However, it cannot be used to investigate HFs with complex cladding configurations.

Another technique that has been recently developed that can predict confinement loss is based on representing the refractive index distribution as a series of wedges [26]. The field is decomposed within a circular boundary that encloses the holes, and by using continuity conditions at this boundary, the complex propagation constant is calculated using an iterative procedure. The use of wedges allows the overlap integrals between the structure and the field components to be done directly, and so this method can be efficient. In addition, it should ultimately be possible to represent arbitrary fibre profiles in this way.

3 High nonlinearity HFs

One of the most exciting possibilities for applications of HFs is in the development of high effective nonlinearity fibres. In these fibres small core dimensions are coupled with a large contrast between the core and cladding indices to produce extremely tight modal confinement (see for example Fig. 1(b)). Such fibres promise the development of compact devices based on nonlinear effects that can operate at low powers. Some recent examples include devices for optical switching/regeneration [27] and Raman amplification [28].

Small-core HFs pose a number of challenges for effective modelling. The high index contrast inherent in these fibres necessitates the use of a full-vector method. In addition, any imperfections in the fibre profile, when combined with this large contrast and the small structure-scale can lead to significant form birefringence. For example, the fibre shown in Fig. 1(c) is highly birefringent due to the elliptical shape of the core, with a measured beat length of 0.3mm, and a polarisation extinction ratio of 18dB at 1550nm. Using the actual fibre profile in the hybrid orthogonal function method, a beat of length of 0.28mm is predicted, in good agreement with the measured value. By numerically calculating the deviation of the polarisation of the predicted mode from linear, the model predicts an upper bound on the extinction ratio of 19dB, again in good agreement with observations. In general, even small asymmetries can led to noticeable birefringence for these small-core fibres. Hence it is often necessary to use the detailed fibre profile in order to make accurate predictions.

Another property that can play an important role in small-core fibres is confinement loss. This is clear from Fig. 2, which shows predictions of the multipole method for some small-core HFs with hexagonally arranged holes. At small hole-to-hole spacings (Λ), the loss increases as the mode can *see over* the structure into the solid jacket region of the fibre, resulting in loss due to leakage of the mode. Unsurprisingly, confinement loss can always be reduced by using more rings of holes in the cladding. Hence for small-scale structures there is a trade-off between fabrication difficulties and loss. Notice that a relatively small change in Λ can lead to a significant change in the confinement loss. However, using results like those shown in Fig. 2, it is possible to design and fabricate practical low-loss high nonlinearity HFs.

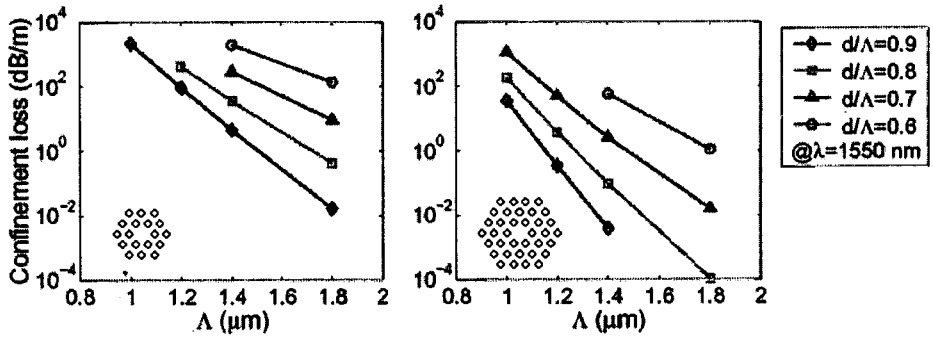

Figure 2: Confinement loss predicted by the multipole method for a range of small-core pure-silica HFs.

4 Large mode area HFs

HFs offer an alternative route towards large mode areas, offering broadband single-moded guidance. Large mode HFs (LMHFs) can be produced either by using a relatively large hole-to-hole spacing ($\Lambda > 5\,\mu$m) and/or small air holes ($d/\Lambda < 0.2$). The models described in Section 2 can be applied to investigate the optical properties of these

fibres, although often extra care is needed due to the wide range of spatial scales present. Polarisation effects are typically less important in this class of fibres, and it is often sufficient to use a scalar model.

Macroscopic bend loss ultimately limits the practically of such large mode fibres, and so understanding bend loss is important in the design of this class of fibre. HFs possess a bend loss edge at short wavelengths in addition to the conventional long wavelength loss edge [11]. Although standard telecommunications wavelengths fall on the short wavelength loss edge for large mode holey fibres [29], these fibres possess comparable bending losses to similarly sized conventional fibres at this wavelength [30].

Two distinct bend loss mechanisms have been identified in conventional fibres; transition loss and pure bend loss [31]. As light travels into a curved fibre, the mode distorts, causing a transition loss (analogous to a splice loss). Pure bend loss occurs continually along any curved section of fibre: at some radial distance (r_c in Fig 3(d)), the tails of the mode need to travel faster than the speed of light to negotiate the bend, and are thus lost. Conventional methods for calculating pure bend loss have been applied to holey fibres via an equivalent step index model with some success for small d and Λ [11, 29]. Transition and pure bend losses can be distinguished experimentally [31] by progressively wrapping a fibre around a drum of radius R_0. The fibre experiences a sharp change of curvature as it enters and leaves the drum surface, which results in transition losses at these points. As the angle is increased, the length of the curved section (and the pure bend loss) increases linearly. Figure 3 shows the measured loss as a function of angle for $R_0 = 14.5$ mm. Each data set shows two regions: the curved section of each plot is the transition region, while the pure bend loss dominates as the length of the bent fibre increases. Results for two different angular orientations of the same fibre illustrate that the geometry of the cladding structure has a noticeable effect on the bend loss characteristics, and so any effective index method will paint an incomplete picture.

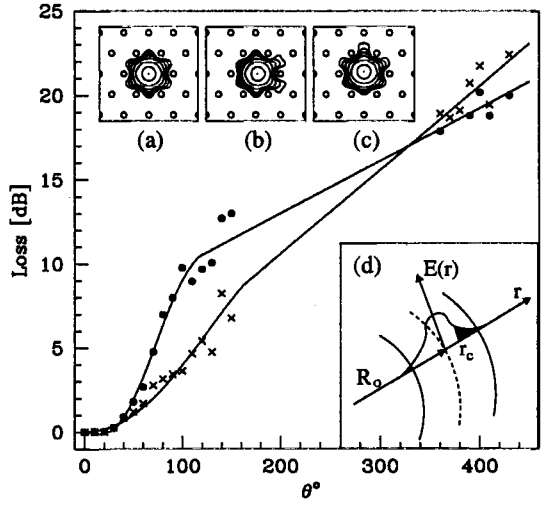

Figure 3: Loss as a function of angle for two fibre orientations (see text and [31]) for the HF in Fig. 1(a). (a) Calculated mode profile for HF, (b) and (c): calculated mode for a bend in horizontal and vertical directions respectively (contours every 2dB), (d): slice through mode propagating around bend of radius R_0.

One way of modelling the propagation of light in a fibre with a radius of curvature R_0 is to scale the refractive index using the transformation: $\sqrt{(1 + (2r\,cos\alpha)/R_0)}$, where the coordinates are defined in Ref [32]. The modes of the bent microstructured fibre can then be calculated using one of the techniques described in Section 2.2 (note that the slant introduced by this transformation can not be described in all of the models: for example the super-cell plane wave method and multipole methods cannot be used). To calculate the modes shown in Fig. 3 the hybrid orthogonal function model was used: modal intensities are shown in Fig 3 for (a) a straight fibre, and (b) and (c) for fibre bent in horizontal and vertical directions respectively. Using these modes, we calculate the transition loss as the overlap between the straight and bent modes, and for pure bend loss we assume that the fraction of energy in the guided mode at $r > r_c$ is lost over some distance scale. This model allows trends relating to the angular orientation of the fibre to be identified.

5 Conclusion

A number of techniques have been adapted or developed to model microstructured optical fibres, and a range of novel guidance regimes have been identified in these fibres that promise to lead to a new generation of optical devices with tailor-made optical properties. Many of the techniques described herein complement one another and can be used in conjunction to obtain a complete picture of the optical characteristics of any given microstructured fibre. The extremes that are possible in these fibres have highlighted a number of challenges in accurate modelling of their properties, and it seems likely that as the technology for fabricating these structures matures further challenges will emerge.

References

[1] J.C. Knight, T.A. Birks, P.St.J. Russell, and M. Atkin, Opt. Lett. **21**, 1547 (1996).

[2] T.A. Birks, P.J. Roberts, P.St.J. Russell, D.M. Atkin and T.J. Shepherd, Elect. Lett. **31**, 1941 (1997).

[3] R.F. Cregan, B.J. Mangan, J.C. Knight, T.A. Birks, P.St.J. Russell, P.J. Roberts and D.C. Allan, Science **285**, 1537 (1999).

[4] T.M. Monro, P.J. Bennett, N.G.R. Broderick and D.J. Richardson, Opt. Lett. **25**, 206 (2000).

[5] W.J. Wadsworth, J.C. Knight, W.H. Reeves, P.St.J. Russell, J. Arriaga, Electron. Lett. **36**, 1452 (2000).

[6] K. Furusawa, T.M. Monro, P. Petropoulos, D.J. Richardson, Electron. Lett. **37**, 560 (2001).

[7] T.M. Monro, Y.D. West, D.W. Hewak, N.G.R. Broderick and D.J. Richardson, Electron. Lett. **36** 1998, (2000).

[8] M.A. van Eijkelenborg, M.C.J. Large, A. Argyros, J. Zagari, S. Manos, N. Issa, I. Bassett, S. Fleming, R.C. McPhedran, C.M. de Sterke and N.A.P. Nicorovici, Optics Express **9**, 319 (2001).

[9] T.M. Monro, D.J. Richardson, N.G.R. Broderick and P.J. Bennett, J. Lightwave Technol., **17**, 1093 (1999).

[10] N.G.R. Broderick, T.M. Monro, P.J. Bennett and D.J. Richardson, Opt Lett. **24**, 1395 (1999).

[11] J.C. Knight, T.A. Birks, R.F. Cregan, P.St.J. Russell and J.P. de Sandro, Elect. Lett. **34**, 1347 (1998).

[12] T.A. Birks, J.C. Knight and P.St.J. Russell, Opt. Lett. **22**, 961 (1997).

[13] J.C.Knight, J. Arriaga, T.A. Birks, A. Ortigosa-Blanch, W.J. Wadsworth and P.St.J. Russell, IEEE Phot. Tech. Lett. 12, 807–809 (2000).

[14] T.M. Monro, V. Pruneri, N.G.R. Broderick, D. Faccio, P.G. Kazansky and D.J. Richardson, IEEE Phot. Tech. Lett. , 981 (2001).

[15] T.P. White, R.C. McPhedran, C.M. de Sterke and L.C. Botten, Opt. Lett. **26**, 1660 (2001).

[16] T.A. Birks, D. Mogilevtsev, J.C. Knight and P.St.J. Russell, IEEE Phot. Tech. Lett. **11**, 674 (1999).

[17] J. Riishede, S.B. Libori, A. Bjarklev, J. Broeng and E. Knudsen, Proc. 27th European Conference on Optical Communication (ECOC' 2001), Th.A.1.5 (2001).

[18] T.M. Monro, D.J. Richardson, N.G.R. Broderick and P.J. Bennett, J. Lightwave Technol. **18**, 50 (2000).

[19] B.J. Eggleton, P.S. Westbrook, R.S. Windeler, S. Spalter and T.A Strasser, Opt. Lett. **24**, 1460 (1999).

[20] E. Silvèstre, M.V. Andrés and P. Andrés, J. Lightwave Technol., **16**, 923 (1998).

[21] J.Broeng, S.E. Barkou, T. Sondergaard and A. Bjarklev, Opt. Lett. **25**, 96 (2000).

[22] D. Mogilevtsev, T.A. Birks and P.St.J. Russell, Opt. Lett. **23**, 1662 (1998).

[23] T.M. Monro, N.G.R. Broderick, and D.J. Richardson, M. Bertolotti, C.M. Bowden and C. Sibilia, eds. in *Nanoscale, linear and nonlinear optics* (Vol 560 of International School on Quantum Electronics), 123 (2000).

[24] P.J. Bennett, T.M. Monro and D.J. Richardson, Opt. Lett. **24**, 1203 (1999).

[25] M.J. Steel, T.P. White, C.Martijn de Sterke, R. McPhedran, L.C. Botten, Opt. Lett. **26**, 488 (2001).

[26] L. Poladian and T.M. Monro, Proc. Australian Conference on Optics and Lasers (ACOLS' 2001), Th(b)3 (2001).

[27] P. Petropoulos, T.M. Monro, W. Belardi, K. Furusawa, J.H. Lee and D.J. Richardson, Opt. Lett. **26**, 1233 (2001).

[28] J.H. Lee, Z. Yusoff, W. Belardi, T.M. Monro, P.C. Teh and D.J. Richardson, Proc. 27th European Conference on Optical Communication (ECOC' 2001), PD.A.1.1, 46 (2001).

[29] T. Sorensen, J. Broeng, A. Bjarklev, E. Knudsen, and S.E. Barkou Libori, Elect. Lett. **37**, 287 (2001).

[30] J.C.Baggett, T.M.Monro, K.Furusawa and D.J.Richardson, Opt. Lett. **26**, 1045 (2001).

[31] W.A. Gambling, H.Matsumura, C.M. Ragdale, and R.A. Sammut, Microwaves, optics and acoustics **2**, 134 (1978).

[32] D. Marcuse, Appl. Opt. **21**, 4208 (1982).